Published in Applied Physics Letters 75, 3769-3771, 1999
which should be used for any reference to this work

Surface-emitting 10.1 μm quantum-cascade distributed feedback lasers

Daniel Hofstetter,[a] Jérôme Faist, and Mattias Beck
University of Neuchâtel, Institute of Physics, 1 Rue A.-L. Breguet, Neuchâtel CH 2000, Switzerland

Ursula Oesterle
Swiss Federal Institute of Technology–Lausanne, Institute of Micro- and Optoelectronics, Physics Department, PHB Ecublens, CH 1015 Lausanne, Switzerland

We present measurement results on a surface-emitting quantum-cascade distributed feedback laser emitting infrared radiation at 10.1 μm. The use of a second order grating enabled the laser to emit about 25% of its total optical power from the grating. The beam radiated from the grating was at a very low divergence angle of about $1°\times14°$. As already presented in a previous paper, we simplified the processing by using a lateral current injection scheme avoiding epitaxial regrowth. At 85 K, the laser emitted 210 and 60 mW of pulsed power from facet and grating, respectively; at room temperature, the corresponding numbers were 70 and 18 mW. Threshold current densities of 2.1 kA/cm^2 at 85 K and 5.6 kA/cm^2 at room temperature were observed. The device showed single mode behavior for the entire temperature range and all investigated power levels. In addition, a constant temperature tuning coefficient of 0.06 cm^{-1}/K was seen.

Quantum cascade (QC) lasers are very promising light sources for micro-optical environmental sensors in the mid-infrared spectral region.[1–3] For many of those applications, however, the availability of a surface-emitting laser would greatly facilitate the coupling of the light into the optical system. Since, for fundamental reasons (TM polarization), a QC laser cannot be configured as a vertical cavity surface-emitting laser, other methods to achieve surface emission have to be pursued. An additional desired property of a light source for sensors is its single-mode behavior even in pulsed operation and at high power levels. In order to achieve single-mode operation, distributed feedback (DFB) QC lasers have been already extensively investigated and characterized.[4–6] An elegant and, up to this point, unexplored method to obtain surface emission is the fabrication of a DFB QC laser utilizing a second order diffraction grating.[7] This has the additional advantage that the grating with a period of around 3.15 μm can be fabricated by moderate-solution contact lithography instead of holography. Accordingly, we will present here recent results about a surface-emitting second order DFB laser at 10.1 μm. Although DFB lasers have obvious performance benefits, they usually suffer from the fact that epitaxial regrowth is necessary to complete the structure after grating fabrication. As has been recently demonstrated, one can use a lateral current injection scheme in order to fabricate a strongly coupled, low loss grating without epitaxial regrowth. These devices have a waveguide with a semiconductor lower cladding and air forming the top cladding. The heavily *n*-doped InGaAs cap layer, which serves as host layer for the grating, is highly conducting to allow lateral current injection and distribution throughout the device. Important consequences of such a design are that there is a large refractive index step between semiconductor and air, and that there are low calculated losses of 12 cm^{-1}. This results in both a high coupling coefficient of the grating and a relatively high net gain of the laser; thus it potentially allows the fabrication of short devices with a low threshold current.

Growth of this material was based on molecular beam epitaxy (MBE) of lattice matched $In_{0.53}Ga_{0.47}As$/$In_{0.52}Al_{0.48}As$ layers on top of an *n*-doped InP (Si, 2×10^{17} cm^{-3}) substrate. The growth process started with the lower waveguide layer ($In_{0.53}Ga_{0.47}As$, Si, 6×10^{16} cm^{-3}, thickness 1.25 μm), proceeded with an active region (thickness 1.75 μm) and was finished by a thicker upper waveguide layer ($In_{0.53}Ga_{0.47}As$, Si, 6×10^{16} cm^{-3}, thickness 2.1 μm) and a 0.7 μm thick highly *n*-doped cap layer on top ($In_{0.53}Ga_{0.47}As$, Si, 2×10^{18} cm^{-3}). The active region, which thus formed the central part of the waveguide, consisted of 35 superlattice periods; those were alternating *n*-doped funnel injector regions and undoped triple quantum well active regions. The laser transition in the latter was diagonal, as described in Ref. 8. The layer sequence of the structure, in nanometers, starting from the injection barrier, is as follows: 3.9/**1.0**/3.8/**1.2**/3.7/**1.5**/3.9/**1.7**/4.0/**4.2**/3.1/**0.9**/6.4/**1.0**/6.0/**2.8** nm. $In_{0.52}Al_{0.48}As$ layers are in bold, $In_{0.53}Ga_{0.47}As$ layers are in roman, and *n*-doped layers (Si 2.5×10^{17} cm^{-3}) are underlined.

The fabrication of these second order DFB lasers was based on holographically defining a grating with 3.15 μm period ($n_{\text{eff}}=3.22$), and wet chemical etching of the grating in a $H_2SO_4/H_2O_2/H_2O$ (1:8:1) solution to a depth of 0.6 μm (etch rate ~100 nm/sec). We used a 488 nm Ar-ion laser and a 90° corner reflector mounted on a rotational stage for the grating exposure. The grating lines run along the dove-tail direction of the crystal in order to achieve a nonrectangular tooth profile and to obtain a sufficiently high first order Fourier component. This is quite critical for device performance because a symmetric rectangular second order grating contains no first order Fourier component. Unfortunately, grat-

[a]Electronic mail: Daniel.Hofstetter@iph.unine.ch

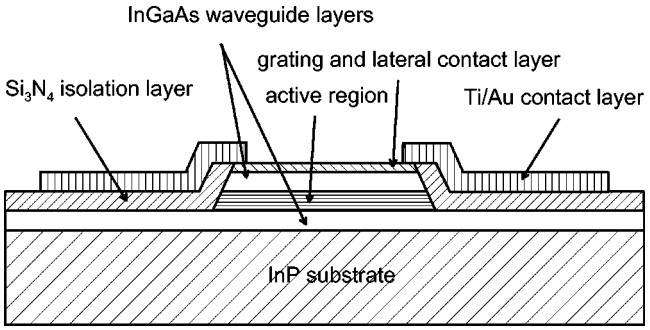

FIG. 1. Schematic cross section through the laser waveguide showing the position of the grating with respect to the active layer and the metal top contact.

ing fabrication by holography and wet etching usually results in underetching and leads to narrow grating lines and large spaces between them (duty cycle <50%, see inset of Fig. 3). Because a small duty cycle reduces the average refractive index and therefore the overlap factor of the grating layer, the coupling coefficient and the diffraction efficiency of the grating become small, resulting in a limited amount of surface-emitted power.

Standard processing techniques were used to define ridge waveguides with a width of 35–55 μm (etch depth 4.5 μm, etch depth 4.5 μm, $HBr/HNO_3/H_2O$, 1:1:10, etch rate 800 nm/min) and a length of 1–1.5 mm.[3] 300 nm of Si_3N_4 served as an electrical passivation layer and Ti/Au (10/400 nm) was used as the top contact metal. Thinning, back contacting (Ge/Au/Ag/Au, 12/27/50/100 nm), and cleaving completed the processing. As shown by the schematic cross section in Fig. 1, the contact metal covered only the edges (about 5 μm on each side) of the ridge to prevent large absorption losses in the waveguide, but still allow lateral current injection. The devices, whose facets were left uncoated, were mounted ridge side up on copper heatsinks and operated at different temperatures between 85 and 300 K. For this purpose, the samples were placed into a temperature controlled N_2 flow cryostat. The light from the facet of the DFB QC laser was collected by $f/0.8$ optics and fed into a high resolution Fourier transform spectrometer (Nicolet type Magna-IR 860), where we detected it using a liquid nitrogen-cooled HgCdTe detector. For the measurement of light versus current ($L-I$) curves, we measured the intensity with a calibrated 500×500 μm^2 room temperature HgCdTe detector. Typical edge emission $L-I$ and current versus voltage ($I-V$) curves of a 55 μm wide and 1.125 mm long device are shown in Fig. 2. The current pulses were 100 ns long, and a pulse repetition frequency of 5 kHz was used for all temperatures. At low temperatures, we observed a threshold current of 1.3 A and a maximum output power of 210 mW from the facet. The slope efficiency at this temperature was 105 mW/A and a threshold current density of 2.1 kA/cm^2 was determined. At room temperature, we obtained 70 mW optical output power from the facet, with a slope efficiency of 70 mW/A. However, the threshold current increased to 3.45 A (threshold current density of 5.6 kA/cm^2), and an operating voltage of 10.5 V was seen. From the increase in threshold current, we were able to derive a characteristic temperature T_0 of 258 K. The higher slope efficiencies at 150 and 200 K (compared to 85 K) are due to the fact that

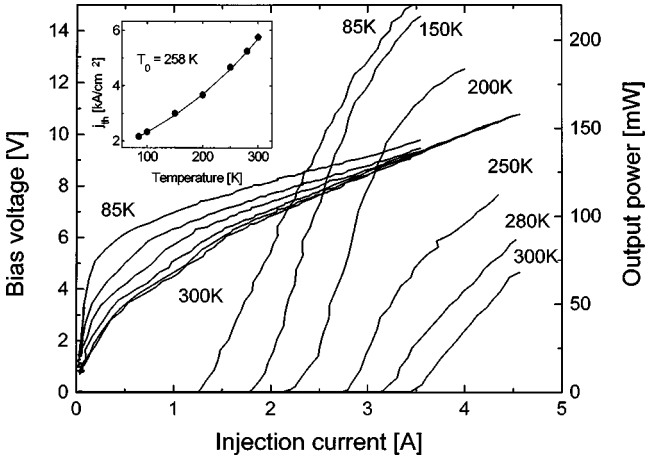

FIG. 2. $L-I$ and $I-V$ curves of a 55 μm wide and 1.125 mm long second order DFB QC laser measured at different temperatures (edge emission). The inset shows a plot of the threshold current vs. device temperature.

the grating resonance wavelength is tuned at the center of the gain peak at these temperatures. This explains also the higher T_0 value of these devices than our previously published DFB lasers.[5]

Figure 3 shows a comparison between the $L-I$ characteristics for both facet and grating emission. Because of the unfavorable duty cycle of the grating (about 0.25–0.35 instead of 0.7), there is a bigger fraction of the total energy radiated from the facet than from the grating. Nevertheless, we obtained an optical output power from the grating of 60 mW at 85 K and 18 mW at 300 K; these values correspond to quantum efficiencies of 30 and 18 mW/A, respectively. In Fig. 4, we present the far field distribution of the grating emission in both directions. In the direction along the waveguide, we observed, due to the wide aperture and the Bragg reflection, a very narrow far field angle of about 1° full width at half maximum (FWHM), whereas in the other, perpendicular direction, the far field angle was equivalent to the one observed at the corresponding direction of the facet, namely about 14° (FWHM).

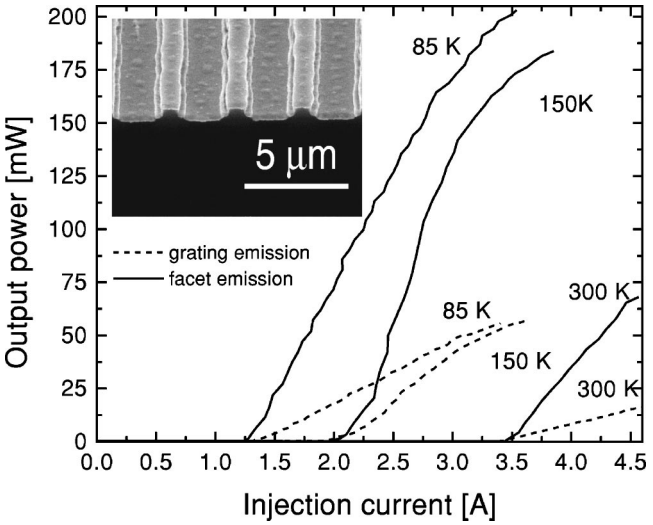

FIG. 3. Comparison between $L-I$ curves with the output intensity collected from the facet and the grating at three representative temperatures. The inset shows a scanning electron microscope image of the grating.

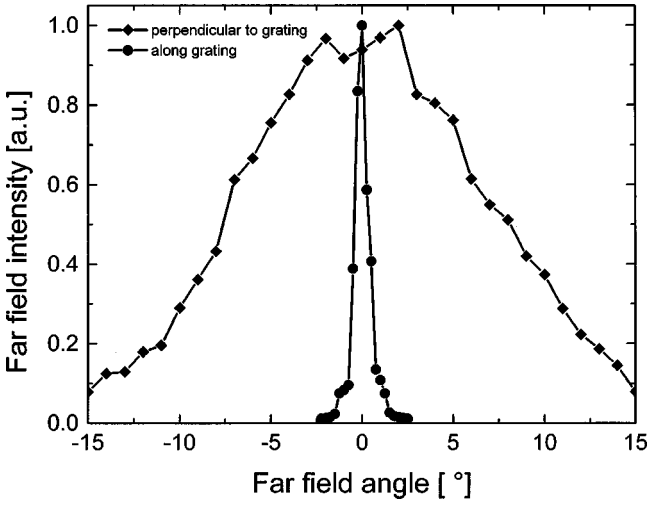

FIG. 4. Far field distributions of the surface emission from a second order DFB QC laser measured in two orthogonal directions (along and perpendicular to the waveguide).

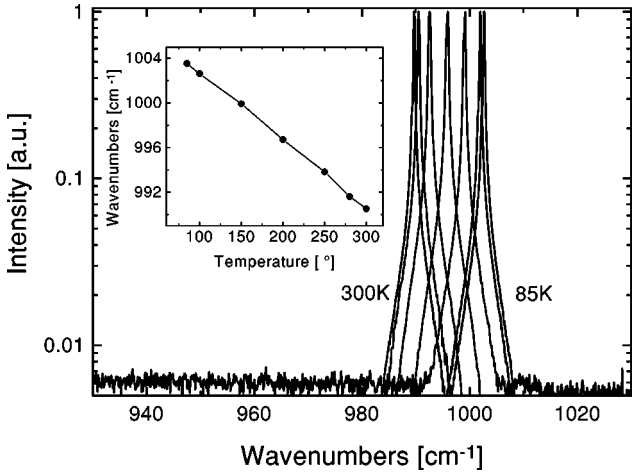

FIG. 5. Lasing spectra of a 55 μm wide and 1.125 μm long DFB QC laser at different temperatures between 85 and 300 K. The inset shows the linear tuning of the wavelength with temperature.

According to Ref. 9, a certain amount of gain/loss coupling is always present in a second order DFB laser. This loss coupling should prevent the device from oscillation in both stop-band modes. Most likely because of their relatively weak coupling coefficient, we observed, on short devices and at high injection currents, lasing action in both stop-band modes. This allowed us a relatively precise measurement of the Bragg reflector's stop-band width; the value was $\Delta\lambda = 1.1\ \mathrm{cm}^{-1}$. From this figure, we determined the coupling coefficient of the grating to be $\kappa = \Delta\lambda\pi n_{\mathrm{eff}}/\lambda^2 = 12\ \mathrm{cm}^{-1}$; with n_{eff} being the effective refractive index of the propagating mode. This number is of the same order of magnitude as the calculated value obtained from the effective refractive index difference of $\Delta n_{\mathrm{eff}} = 1.8\times10^{-2}$ between areas with and without the grating layer ($\kappa = \pi\Delta n_{\mathrm{eff}}/2\lambda = 9\ \mathrm{cm}^{-1}$) and the first Fourier component of the grating teeth. A relatively small free carrier absorption loss of 12 cm^{-1} was calculated for this device, whereas a laser utilizing our standard waveguide design with a 2.2 μm thick InAlAs/InGaAs upper cladding layer and a metal-covered grating would suffer from a waveguide loss of 30 cm^{-1}. In addition, the refractive index contrast would be reduced by almost two orders of magnitude, namely to a value of $\Delta n_{\mathrm{eff}} = 2.3\times10^{-4}$.

Finally, Fig. 5 shows the lasing spectra at temperatures between 85 and 300 K. We observed single mode operation for all temperatures and, in particular, at maximum power for each individual temperature. We determined the linewidth to be on the order of 0.3 cm^{-1}, which corresponds to the resolution limit of our experimental setup. The emission wavelength at 85 K was 1004 cm^{-1}; at room temperature, it decreased to 990 cm^{-1}. The luminescence peak was found in the vicinity of 1000 cm^{-1} for all temperatures. The temperature tuning coefficient of the lasing peak was constant over the entire temperature range, and its magnitude was $1/\lambda \times \Delta\lambda/\Delta T = 6.1\times10^{-5}\ \mathrm{K}^{-1}$ ($\Delta\nu/\Delta T = -0.06\ \mathrm{cm}^{-1}/\mathrm{K}$).[5]

In conclusion, we have shown device results for a second order, surface emitting DFB QC laser operating at 10.1 μm. At room temperature, the laser emitted 70 mW optical power through the facet and 18 mW from the grating into a single mode. The corresponding numbers for 85 K were 210 and 60 mW for facet and grating emission, respectively. Pulsed threshold current densities of 5.6 and 2.1 $\mathrm{kA/cm}^{-2}$ were seen for 300 and 85 K, respectively. The far field angle of the surface emission was 1°×14°.

The authors would like to thank Stéphane Blaser and Antoine Müller for their help; and the Swiss National Science Foundation and the Science Foundation of the European Community under Contract BRITE/EURAM Project UNISEL (Contract No. CT97-0557) for their financial support.

[1] J. Faist, F. Capasso, D. L. Sivco, A. L. Hutchinson, and A. Y. Cho, Science **264**, 553 (1994).
[2] J. Faist, F. Capasso, C. Sirtori, D. L. Sivco, J. N. Baillargeon, A. L. Hutchinson, S. N. G. Chu, and A. Y. Cho, Appl. Phys. Lett. **68**, 3680 (1996).
[3] C. Sirtori, J. Faist, F. Capasso, D. L. Sivco, A. L. Hutchinson, and A. Y. Cho, Appl. Phys. Lett. **68**, 1745 (1996).
[4] J. Faist, C. Gmachl, F. Capasso, C. Sirtori, D. L. Sivco, J. N. Baillargeon, and A. Y. Cho, Appl. Phys. Lett. **70**, 2670 (1997).
[5] D. Hofstetter, J. Faist, A. Müller, M. Beck, and U. Oesterle, Appl. Phys. Lett. **75**, 665 (1999).
[6] C. Gmachl, F. Capasso, J. Faist, A. L. Hutchinson, A. Tredicucci, D. L. Sivco, J. N. Baillargeon, S. N. G. Chu, and A. Y. Cho, Appl. Phys. Lett. **72**, 1430 (1998).
[7] G. A. Evans, D. P. Bour, N. W. Carlson, J. M. Hammer, M. Lurie, J. K. Butler, S. L. Palfrey, R. Amantea, L. A. Carr, F. Z. Hawrylo, J. B. Kirk, S. K. Liew, and W. F. Reichert, Appl. Phys. Lett. **55**, 2721 (1989).
[8] J. Faist, C. Sirtori, F. Capasso, D. L. Sivco, J. N. Baillargeon, A. L. Hutchinson, and A. Y. Cho, IEEE Photonics Technol. Lett. **10**, 1100 (1998).
[9] W. Streifer, R. D. Burnham, and D. R. Scifres, IEEE J. Quantum Electron. **JQE-12**, 737 (1976).